ARTICLE

Rapid Silica Atomic Layer Deposition on Large Quantities of Cohesive Nanoparticles

Xinhua Liang,[†] Kathryn S. Barrett,[†] Ying-Bing Jiang,[‡] and Alan W. Weimer*,[†]

Department of Chemical and Biological Engineering, University of Colorado, Boulder, Colorado 80309, TEM Laboratory, University of New Mexico, Albuquerque, New Mexico 87131

ABSTRACT Conformal silica films were deposited on anatase titania nanoparticles using rapid silica atomic layer deposition (ALD) in a fluidized bed reactor. Alternating doses of tris(tert-pentoxy)silanol (TPS) and trimethylaluminum (TMA) precursor vapors were used at 175 °C. In situ mass spectroscopy verified the growth mechanism through a siloxane polymerization process. Transmission electron microscopy revealed highly conformal and uniform silica nanofilms on the surface of titania nanoparticles. A growth rate of ~1.8 nm/cycle was achieved for an underdosed and incomplete polymerization reaction. Primary nanoparticles were coated despite their strong tendency to form dynamic agglomerates during fluidization. Methylene blue oxidation tests indicated that the photoactivity of anatase titania particles was mitigated with the ALD films.

KEYWORDS: atomic layer deposition (ALD) • silica • nanoparticle • fluidized bed reactor

1. INTRODUCTION

Silicon dioxide (SiO_2) is one of the most important materials used in the production of silicon microelectronic devices and its applications range from gate dielectrics to passivation layers (1). Ultrathin SiO_2 films have been deposited by atomic layer deposition (ALD) (2−5), in which a film grows one monolayer at one reaction cycle with precise atomic layer control. ALD is a surface-controlled layer-by-layer gas phase thin film deposition method (6−8), modified from the CVD technique. In ALD, the film growth takes place in a cyclic manner. The simplest case includes four steps: (1) exposure of the first precursor, (2) purge or evacuation of the reactor chamber, (3) exposure of the second precursor, and (4) purge or evacuation of the reactor chamber. As a consequence of the finite number of reaction sites on the substrate surface, the reactions are self-limiting. Only one monomolecular layer of the precursor becomes firmly bound to the substrate surface with each dose. The film thickness is, therefore, simply determined by the growth rate per cycle and the number of cycles completed. This approach is ideal for growth of ultrathin films. However, the application of ALD is throughput limited for deposition of relatively thick films because of slow deposition rates, with a theoretical maximum of one monolayer per cycle. For several microelectronic and optical applications, thicker dielectric films are desired. Recently, a new SiO_2 deposition method using silanols with catalysts has been developed. It is known as "rapid SiO_2 ALD" (9, 10). Unlike a conventional ALD reaction that produces a monolayer growth, the second half of this reaction includes a catalytic reaction between precursors that leads to significantly thicker film growth per cycle.

Rapid SiO_2 ALD provides for deposition rates that are much higher than those for conventional SiO_2 ALD while still maintaining the self-limiting behavior characteristic of ALD (9). Silanols used for rapid SiO_2 ALD include tris(tert-butoxy)-silanol ($(tBuO)_3SiOH$, TBS) and tris(*tert*-pentoxy)silanol (TPS). Metals such as aluminum (9, 10), zirconium (11) and hafnium (12) have been used as the catalyst for rapid SiO_2 ALD. In a study of the ALD of Al_2O_3/SiO_2 films, Gordon and coworkers discovered that as many as 30 monolayers of SiO_2 could be deposited during a single pulse of $(tBuO)_3SiOH$ (9). The catalytic reaction produces a thicker film growth that involves insertion of $(tBuO)_3SiOH$ into a M-O bond that leads to formation of a siloxane polymer bond (9). The catalytic effect of the Al source is significantly larger than that of the other metal sources (13).

The growth of rapid SiO_2 ALD films on different substrates has been demonstrated (9, 10), however, large scale rapid SiO_2 ALD coating on particles is currently unavailable. Nanoparticles have gained increased interest in a variety of fields for different applications (14). The performance of several nanoparticle applications could be improved when such particles are coated with SiO_2 films. Challenges are encountered during ALD on large quantities of nanoparticles. First, the native cohesive properties of the nanoparticles will form agglomerates that are several times larger than the primary particles. Second, it is difficult to deliver the low-vapor-pressure, bulky organic precursor to the reaction chamber and to subsequently remove the "sticky" precursors from the primary nanoparticle surfaces. Third, the formation of polymer siloxane bonds characteristic of rapid SiO_2 ALD may increase the tendency for particle aggregation compared to the traditional ALD coating process.

* To whom correspondence should be addressed. E-mail: alan.weimer@colorado.edu.

Received for review March 30, 2010 and accepted July 9, 2010

[†] University of Colorado.

[‡] University of New Mexico.

DOI: 10.1021/am100279v

Published on Web 07/21/2010

ALD particle coating has been successfully carried out in a fluidized bed reactor (FBR) (15−17). In the design of an FBR, a porous metal disk is used as a gas distributor and a porous metal filter element is used at the inside top of the reactor column to retain the particles in the reactor at all times. The reactor itself is maintained at a vacuum using a vacuum pump. With appropriate expansion of a bed of particles, granular materials are transformed into a fluid-like state through contact with a gas. The rigorous mixing during fluidization provides excellent fluid solid contacting. The FBR has many advantages, including good mixing, large gas−solid contact area, high efficiency of mass and heat transfer, and large-batch processing capability. The objective for this study was to demonstrate the feasibility of coating large quantities of cohesive nanoparticles with SiO_2 films using rapid SiO_2 ALD in an FBR. For proof of concept, anatase titania nanoparticles of two different particle sizes were used as particle substrates. Rapid SiO_2 ALD was performed using TPS with trimethylaluminum (TMA) providing the Al catalyst in a vibrating FBR.

2. EXPERIMENTAL SECTION

2.1. Rapid Silica ALD on Nanoparticles. The ALD process was carried out in a vibrating FBR, as shown in Figure S1 (see the Supporting Information). This system consists of a reactor column, a vibration generation system, a data acquisition and control system with LabView, and in situ mass spectrometry, which has been described in detail previously (18, 19). The fluidized bed is 3.5 cm in diameter and 110 cm in length. There is a 10 μm pore size porous metal disk in the center of the reactor as the gas distributor. The reactor is encased by a clamshell-type furnace and bolted to a platform that rests on four large springs. A vibration system is utilized to overcome some of the interparticle forces and improve the quality of fluidization. High-purity N_2 gas is used as the purge gas to remove the unreacted precursor and any byproduct formed during the reaction and its flow rate is controlled by a mass flow controller. Baratron capacitance manometers (MKS Instruments) are located below the distributor plate and at the outlet of the reactor column to measure the pressure drop across the bed of particles. All valves used to provide the transient dosing are automatically controlled through LabView (National Instruments). Pressure measurements are recorded to monitor the progress of each dosing cycle. An internal quadrupole mass spectrometer (Stanford Research Systems) was connected to the outlet side of the reactor, as shown in Figure S1 in the Supporting Information.

TMA (97%) and TPS (99.99+ %) were purchased from Sigma Aldrich Company and used as received. Rapid SiO_2 ALD was carried out on two different batches of anatase titania particles (Millennium Chemicals). One has a surface area of 88.0 m^2/g, and the other has a surface area of 9.6 m^2/g. On the basis of the surface area, the corresponding calculated average particle size is 18 and 160 nm, respectively. For a typical run, 10 g of particles were loaded into the reactor. The reaction temperature was 175 °C. The feed lines were kept at ∼100 °C to avoid excessive adsorption of TPS on the internal walls of the system. The minimum pressure inside the reactor was ∼50 mTorr and the minimum fluidization superficial gas velocity (U_{mf}) was determined by measuring the pressure drop across the bed versus the N_2 superficial gas velocity. One example of titania particle fluidization at 175 °C is shown in Figure 1, and the U_{mf} is ∼0.42 cm/s for 10 g 18 nm titania nanoparticles fluidized at 175 °C and reduced pressure. During the ALD reaction, TMA was fed through the distributor of the reactor using its room-temperature vapor pressure to provide for flow. The flow rate of TMA was limited using a needle valve. The room-temperature vapor pressure of TPS is much lower than that required for the fluidization of reasonable bed masses. Heating the TPS liquid raises its vapor pressure. A bubbler was employed to dilute the heated TPS vapor stream and allowed for vapor delivery to the reactor in a controllable fashion, preventing precursor overdose. The bubbler inlet was controlled using a mass flow controller from MKS Instruments to allow a calibrated amount of N_2 to be bubbled through the precursor reservoir. In this case, a flow rate of 3 sccm of N_2 was sufficient to deliver TPS, which was preheated to 130−150 °C, to the reactor.

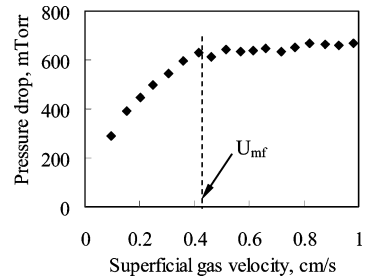

FIGURE 1. Pressure drop across the fluidized bed versus superficial gas velocity for 10 g 18 nm titania nanoparticles at 175 °C and reduced pressure. The minimum fluidization superficial gas velocity (U_{mf}) was determined by measuring the pressure drop across the bed versus the N_2 superficial gas velocity.

In situ mass spectrometry was used to effectively monitor gaseous product evolution and subsequent unreacted precursor breakthrough. The *m*/*z* peaks of interest (i.e., primary and fragmentation peaks) for the precursors were 42, 57, 72 for TMA; 55, 70 for byproduct; 16 for byproduct CH_4; and 18 for byproduct H_2O. This real-time monitoring strategy allows for optimizing the dose time of precursors to prevent process overruns and excess precursor waste. Before the reaction, the particles were dried at 175 °C under continuous N_2 flow for 5 h. A typical coating cycle (10 g of 18 nm titania particles) consisted of the following sequence: TMA dose (10 min), N_2 flush (40 min); TPS dose (30 min), N_2 flush (300 min).

2.2. ALD Coating Characterization. The coated particles were visualized with a JEOL 2010F 200 kV Schottky field emission transmission electron microscope equipped with an Oxford detector unit for elemental analysis while imaging. Inductively coupled plasma-atomic emission spectroscopy (ICP-AES) was performed using an Applied Research Laboratories ICP-AES 3410+. ICP-AES provides the concentration in parts per million (ppm) by mass of silicon and aluminum in relation to the particles. The specific surface area of the particles before and after ALD coating was calculated by the Brunauer−Emmett−Teller (BET) method from the N_2 adsorption isotherms obtained at 77 K (20). The measurements were carried out using a Micromeritics' Gemini V Series Surface Area Analyzer.

2.3. Photoactivity Test by Methylene Blue Oxidation. Methylene blue ($C_{16}H_{18}N_3ClS$, MB) oxidation tests were used in this study to evaluate the passivation effect of the rapid SiO_2 ALD films. For a typical test, 0.1 g of sample particles was dispersed in 100 mL MB aqueous solution having a concentration of 10 ppm. The solution was kept in the dark for 60 min to establish an adsorption/desorption equilibrium condition. For UV irradiation, one UV lamp (Mineralogical Research Co.) of 100 W was used at the distance of 10 cm from the solution. The strength of UV light with a wavelength of 360 nm at the position of the solution surface was measured to be about 10 mW/cm^2 using an IL1400A Radiometer/Photometer (International Light). The solution was continuously stirred during UV irradiation. Concentration of MB in the solution was measured as a function of irradiation time of UV rays. At the given time intervals, analytical samples were taken from the suspension and passed

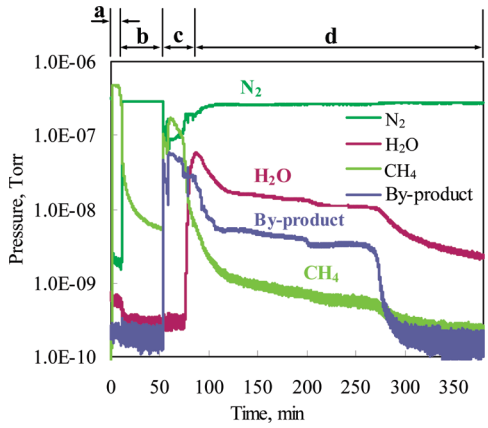

FIGURE 2. In situ mass spectrometry results during one complete cycle of rapid silica ALD on 18 nm titania particles at 175 °C: (a) TMA dose, (b) N_2 flush, (c) TPS dose, and (d) N_2 flush. "By-product" is the signal of *m*/*z* peak 70.

through a 0.2 μm Millipore filter to remove the particles before analysis. The determination of MB concentration was carried out using 2 mL of solution, which was sampled from absorbance change at the wavelength of 664 nm with a Perkin-Elmer Lambda 35 UV/vis/NIR spectrometer.

3. RESULTS AND DISCUSSION

3.1. Rapid Silica ALD through Siloxane Polymerization. The in situ mass spectrometry results of rapid silica ALD on titania particles at 175 °C, shown in Figure 2, reveal the growth mechanism of rapid SiO_2 ALD using TMA and TPS dosing. When TMA was dosed into the reactor, there was an instantaneous increase of the byproduct CH_4. Because the pressure of the reaction product remained relatively constant, the methane generation rate was stable. It is clear that all TMA entering the reactor was completely utilized. With further dose of TMA into the reactor, the CH_4 signal began to decrease, which means that most of the surface reaction was completed. At this point, the TMA dose was stopped, and N_2 was fed into the reactor at a flow rate of 5 sccm to flush any residual reaction product or unreacted TMA from the system. After the 40 min of N_2 flush, TPS was dosed and the CH_4 signal increased again. As the TPS dose proceeded, the reaction byproduct CH_4 began to decrease, and the signal of H_2O (m/z = 18) appeared, which indicated the initiation of the polymerization process. At this point, the TPS dose was stopped, and N_2 was fed into the reactor. The polymerization process continued with the generation of H_2O. At the point when the TPS dose was stopped, the signal of byproduct (e.g., m/z = 18) dropped significantly, which indicates that full surface conversion may not have been obtained. This underdosing was intentional, in order to minimize the amount of unreacted TPS that flowed through the system. During both precursor doses, it is apparent that the reactions were self-limiting, because the reaction products increased and then decreased while the reactants were still being dosed.

The observation of water signal directly supported the previously proposed siloxane polymerization process (9, 10). George and co-workers proposed the mechanism of siloxane polymerization in rapid SiO_2 ALD using TPS and TMA, as listed through eqs 1−4 (10). In this polymerization process, TMA reacts with hydroxylated sites available on the substrate surfaces as given by the reaction in eq 1. Subsequently, the silanols react at the Al center to release CH_4 as expressed by the reaction in eq 2. Additional silanol precursors then can insert at the Al catalytic center and release tert-pentanol, as long as the silanol precursors can diffuse to the Al catalyst (9). In the cross-linking polymerization reactions, the tert-pentoxy ligands eliminate isopentylene and leave behind hydroxyl groups, as indicated in eq 3. Subsequently, the hydroxyl groups can combine to yield H_2O and cross-linking siloxane bonds that terminate the SiO_2 growth, as given by the reaction, eq 4.

$$SiOH^* + Al(CH_3)_3 \rightarrow SiOAl(CH_3)_2^* + CH_4 \quad (1)$$

$$SiOAlCH_3^* + (CH_3CH_2(CH_3)_2CO)_3SiOH \rightarrow SiOAlOSi(OC(CH_3)_2CH_2CH_3)_3^* + CH_4 \quad (2)$$

$$-OSi(OC(CH_3)_2CH_2CH_3)_3^* \rightarrow -OSiOH^* + H_2C=CCH_3CH_2CH_3 \quad (3)$$

$$2SiOH^* \rightarrow Si-O-Si + H_2O \quad (4)$$

As shown in Figure 2, H_2O was continuously generated for 3 h after the TPS dose stopped. The feed lines and the particle bed were flushed for as long as 5 h after the TPS dose. Normally, the polymerization process is fast. The continuous regeneration of H_2O was caused by the continuous feeding of TPS precursor that was swept from the feed tube lines. Though the feed lines were kept at ~100 °C, there was a significant amount of TPS precursor sticking or accumulated within the lines. This was indicated by the significantly higher pressure within the feed zone measured using a Baratron capacitance manometer. Therefore, the continuous and stable feed of TPS precursor into the reactor is a key consideration for this kind of reaction. Low vapor pressure and the sticky tendency of the TPS precursor made this a challenge. Though it was intentionally underdosed, as long as 5 h was required to remove the TPS molecules sticking on the wall of the feed lines.

The concentration of aluminum and silicon on the rapid SiO_2 ALD coated 18 nm particles was measured using ICP-AES. The concentration of aluminum and silicon increased with the increase in the number of ALD coating cycles as shown in Figure 3. As expected, the concentration of aluminum and silicon did not increase linearly versus the number of coating cycles because of the high film growth rate compared to the small particle size of the substrate. There is a constant and high growth rate for rapid silica ALD films and a linear dependence between the film thickness and the number of growth cycles. The molar ratio of Si/Al ranges from 1.3 to 1.7, indicating a high concentration of alumina in the silica films. Previous studies demonstrated

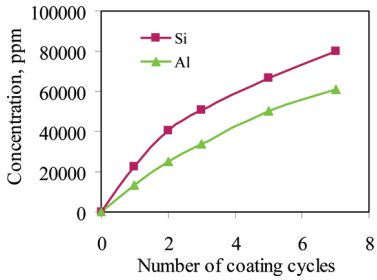

FIGURE 3. Silicon and aluminum concentrations on 18 nm titania particles versus the number of coating cycles.

that <1 at % aluminum existed in the fabricated rapid silica ALD films using TBS and TMA (9). However, a similar high concentration of aluminum or other metal catalyst has been reported by others (11, 12). In this study, the much higher aluminum concentration was most likely the result of intentional underdosing of TPS, which resulted in the lower concentration of silicon.

3.2. Conformal Rapid Silica ALD Films on Particle Surfaces. Rapid silica ALD films have been coated on two different sizes of anatase titania nanoparticles. Transmission electron microscopy (TEM) images of the 160 nm titania particles coated with 3 cycles at a reaction temperature of 175 °C show the presence of extremely conformal ALD films, as displayed in Figure 4. As determined by energy dispersive spectrometry (EDS) elemental nanoanalysis, the films were mainly composed of silicon and aluminum (Figure S2, see the Supporting Information). It is clearly shown in Figure 4a that every particle was coated with a conformal film, and the overlap of the particles clearly indicated that there was no significant particle aggregation. Additional TEM images of the uncoated and 3 cycles of rapid silica ALD coated 160 nm titania particles are shown in Figure S3 (see the Supporting Information). Two batches of the samples were analyzed by TEM and at least 5 particles were analyzed for each batch. The measured thickness of the film is 5.5 ± 0.8 nm, which represents a growth rate of ~1.8 nm/cycle at 175 °C. This growth rate is much slower than the literature value of 12 nm/cycle (10). It is believed that the much slower film growth rate resulted from the intentional underdosing of TPS in this study.

Strong interparticle forces exist between cohesive nanoparticles. It has been shown that nanoparticles fluidize as micrometer-sized agglomerates (21−23). The key challenge in trying to individually coat primary nanoparticles is to overcome their natural tendency to form soft agglomerates. One method to verify that nanoparticles are coated individually is the determination of the surface area. If nanoparticles were coated as aggregates, the surface area would drastically decrease. BET surface area was measured to ensure that the coating did not permanently bind the individual particles into aggregates. Nevertheless, there is an expected change in the surface area of the nanoparticles as the density and the particle size will change as the thickness of the ALD films increases. With the increasing thickness of ALD films, the particle size is larger, which would result in smaller surface area. However, with thicker ALD films, the density of the coated particles would decrease, because the density of titania substrate is larger than that of the combination of silica and alumina. The result is a higher surface area. Therefore, the surface area of the particles could increase or decrease with the increase in the number of ALD coating cycles. With the assumption that the ALD films are the combination of Al_2O_3 and SiO_2, the surface area of the nanoparticles after ALD coating can be estimated using the measured aluminum and silicon concentration on the particle surface, an Al_2O_3 density of 3.5 g/cm^3, a SiO_2 density of 2.2 g/cm^3, and with an ALD film growth rate of 1.8 nm/cycle. The predicted change in surface area for the two different sizes of titania nanoparticles is shown in Figure 5 as a function of ALD film thickness. The predicted surface area for 18 nm titania particles decreases with an increase in the number of ALD coating cycles. In contrast, the predicted surface area of the 160 nm titania particles decreases slightly with an increase in the number of ALD coating cycles for less than six. The surface area of the coated particles begins to increase when the number of coating cycles exceeds six.

The measured surface area of the ALD-coated particles is also displayed in Figure 5. For 160 nm titania particles, the surface area of uncoated particles was 9.6 ± 0.2 m^2/g, and decreased a bit to 9.1 m^2/g after 3 ALD cycles deposited at 175 °C. This is very close to the predicted value. For the 18 nm titania particles, the surface area of the uncoated particles was 88.0 ± 2.0 m^2/g, and decreased with the increase in the number of ALD coating cycles. Experimental and theoretical trends were consistent. These results indicate that nanoparticles were not glued together during the coating process even though TPS is very sticky; the titania nanoparticles are highly cohesive and the coating process includes the polymerization of TPS. The primary particles were coated in the fluidized bed as a result of the tendency for dynamic aggregation (16, 22). Dynamic agglomerates partially break apart and reform because of constant solids recirculation and gas flow through the bed of particles. Even though this breakage is partial and temporary during a single collision event, the entire surface area of each of the primary particles will be eventually exposed and the individual nanoparticles can be coated (16).

3.3. Passivation Effect of Rapid Silica ALD Films. Titania is one of the most widely used white pigments in industrial applications. The use of TiO_2 pigments in industry often involves the incorporation of the pigment into polymeric materials, such as paints and polyolefins. However, TiO_2 is a well-known UV-activated oxidation catalyst, which degrades the polymer surrounding the pigment (24). Coating an ultrathin film on titania particle surfaces is one approach to reduce the photoactivity of TiO_2 particles. The photocatalytic activity of the 160 and 18 nm TiO_2 particles having different thicknesses of rapid silica ALD films deposited at 175 °C is shown in Figure 6. For the uncoated TiO_2 particles, the relative concentration of MB in the solution exponentially decreased with the irradiation time, as reported in the literature (25, 26), and the C/C_0 was almost zero after 90 and 130 min for 18 and 160 nm titania

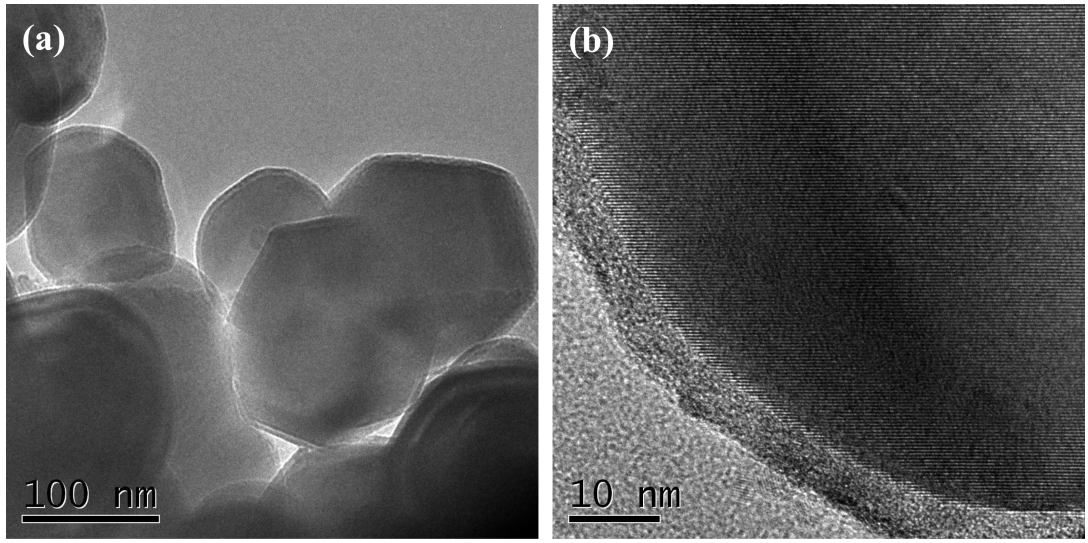

FIGURE 4. (a, b) TEM images of 160 nm titania particles after 3 cycles of rapid silica ALD coating.

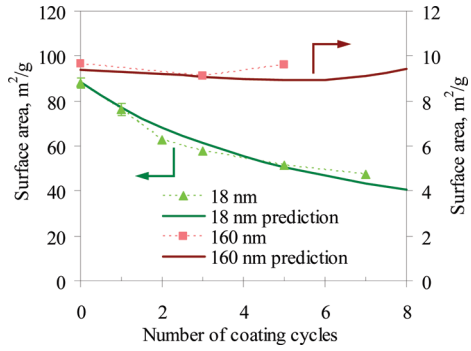

FIGURE 5. Surface area of titania particles versus the number of coating cycles.

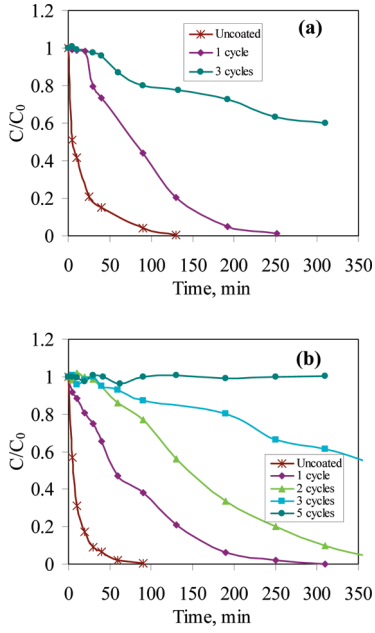

FIGURE 6. Methylene blue concentration in photocatalytic tests as a function of UV irradiation time. (a) 160 nm and (b) 18 nm pigment-grade titania particles were coated with different thicknesses of rapid silica ALD films at 175 °C.

particles, respectively. In contrast, the coated TiO_2 particles showed mitigated photoactivity. For example, for the 160 nm particles of ALD coating with 1 cycle and with 3 cycles, the C/C_0 ratio was 0.21 and 0.78 after 130 min of UV radiation, respectively. For the 18 nm particles coated by ALD using 1, 2, and 3 cycles, the C/C_0 ratio was 0.38, 0.77, and 0.87 after 90 min of UV radiation, respectively; For the particles passivated with 5 cycles of ALD coating, there was no sign of any drop in concentration after over 300 min of UV irradiation. These results demonstrated the conformal coating of rapid silica ALD films on titania nanoparticle surfaces and the effectiveness of the silica coatings to prevent photocatalytic activity on the surface of TiO_2 nanoparticles.

Alumina (27) and silica (28) ALD films and aluminum alkoxide polymer MLD films (29) have been reported for photoactivity mitigation of TiO_2 nanoparticles. Rapid silica ALD films have a similar effect to mitigate photoactivity of TiO_2 nanoparticles. Though the TPS intentionally underdosed, which resulted in a much slower film growth rate, 5 cycles of rapid silica ALD films using TPS and TMA are comparable to 70 cycles of alumina ALD films using TMA and H_2O (29) or 50 cycles of silica ALD films using tris-dimethylaminosilane (TDMAS) and concentrated H_2O_2 (50 wt.% in H_2O) (28). This indicates the high quality of rapid silica ALD films. This large scale rapid silica ALD process has the shortcoming of time issue, but most of the time consumed for this reaction is a long flush or purge time after the dose of TPS. If a full growth rate of 12 nm/cycle is achieved, the time spent to lay down a 12 nm film on particles will be much shorter and 1 cycle of rapid silica ALD film should be capable of mitigating the photoactivity of TiO_2 nanoparticles.

4. CONCLUSIONS

A process for rapid silica ALD coating on large quantities of cohesive nanoparticles has been developed. Primary 18 and 160 nm titania nanoparticles were conformally coated with ultrathin films in a vibrating fluidized bed reactor at 175 °C. In situ mass spectroscopy studies show that the silica ALD film growth was the result of siloxane polymerization

reactions, and the surface reactions were self-limiting. The composition of rapid silica ALD nanolayers was confirmed by EDS. Highly conformal and uniform films on titania nanoparticles were observed via TEM, and the growth rate of rapid silica ALD films was ~1.8 nm/cycle at this experimental condition of underdosing and incomplete polymerization reaction. The thickness of thin films can be effectively controlled by the number of reaction cycles during the sequential vapor deposition process. Though titania nanoparticles are highly cohesive, primary nanoparticles were coated individually due to their dynamic aggregation behavior. This work indicates the feasibility of large scale rapid silica ALD coating on cohesive nanoparticles. Future work will focus on increasing the deposition rate/cycle.

Acknowledgment. The authors thank Millennium Chemicals for providing anatase titania particles and Fredrick G. Luiszer at the University of Colorado for providing the ICP-AES analysis.

Supporting Information Available: Schematic diagram of atomic layer deposition-fluidized bed reactor, EDS spectra, and additional TEM images of uncoated and 3 cycles of rapid silica ALD-coated 160 nm titania particles (PDF). This material is available free of charge via the Internet at http://pubs.acs.org.

REFERENCES AND NOTES

(1) Wilk, G. D.; Wallace, R. M.; Anthony, J. M. *J. Appl. Phys.* **2001**, *89*, 5243–5275.
(2) Klaus, J. W.; Ott, A. W.; Johnson, J. M.; George, S. M. *Appl. Phys. Lett.* **1997**, *70*, 1092–1094.
(3) Klaus, J. W.; Sneh, O.; George, S. M. *Science* **1997**, *278*, 1934–1936.
(4) Ferguson, J. D.; Smith, E. R.; Weimer, A. W.; George, S. M. *J. Electrochem. Soc.* **2004**, *151*, G528–G535.
(5) McCool, B. A.; DeSisto, W. J. *Chem. Vap. Deposition* **2004**, *10*, 190–194.
(6) Suntola, T. *Thin Solid Films* **1992**, *216*, 84–89.
(7) George, S. M.; Ott, A. W.; Klaus, J. W. *J. Phys. Chem.* **1996**, *100*, 13121–13131.
(8) Puurunen, R. L. *J. Appl. Phys.* **2005**, *97*, 121301.
(9) Hausmann, D.; Becker, J.; Wang, S. L.; Gordon, R. G. *Science* **2002**, *298*, 402–406.
(10) Burton, B. B.; Boleslawski, M. P.; Desombre, A. T.; George, S. M. *Chem. Mater.* **2008**, *20*, 7031–7043.
(11) Zhong, L. J.; Chen, F.; Campbell, S. A.; Gladfelter, W. L. *Chem. Mater.* **2004**, *16*, 1098–1103.
(12) Zhong, L. J.; Daniel, W. L.; Zhang, Z. H.; Campbell, S. A.; Gladfelter, W. L. *Chem. Vap. Deposition* **2006**, *12*, 143–150.
(13) He, W.; Solanki, R.; Conley, J. F.; Ono, Y. *J. Appl. Phys.* **2003**, *94*, 3657–3659.
(14) Bruchez, M.; Moronne, M.; Gin, P.; Weiss, S.; Alivisatos, A. P. *Science* **1998**, *281*, 2013–2016.
(15) Wank, J. R.; George, S. M.; Weimer, A. W. *Powder Technol.* **2004**, *142*, 59–69.
(16) Hakim, L. F.; George, S. M.; Weimer, A. W. *Nanotechnology* **2005**, *16*, S375–S381.
(17) Liang, X. H.; Lynn, A. D.; King, D. M.; Bryant, S. J.; Weimer, A. W. *ACS Appl. Mater. Interfaces* **2009**, *1*, 1988–1995.
(18) Liang, X. H.; Hakim, L. F.; Zhan, G. D.; McCormick, J. A.; George, S. M.; Weimer, A. W.; Spencer, J. A.; Buechler, K. J.; Blackson, J.; Wood, C. J.; Dorgan, J. R. *J. Am. Ceram. Soc.* **2007**, *90*, 57–63.
(19) Liang, X. H.; King, D. M.; Li, P.; George, S. M.; Weimer, A. W. *AIChE J.* **2009**, *55*, 1030–1039.
(20) Brunauer, S.; Emmett, P. H.; Teller, E. *J. Am. Chem. Soc.* **1938**, *60*, 309–319.
(21) Wang, Z. L.; Kwauk, M.; Li, H. Z. *Chem. Eng. Sci.* **1998**, *53*, 377–395.
(22) Hakim, L. F.; Portman, J. L.; Casper, M. D.; Weimer, A. W. *Powder Technol.* **2005**, *160*, 149–160.
(23) Quevedo, J. A.; Omosebi, A.; Pfeffer, R. *AIChE J.* **2010**, *56*, 1456–1468.
(24) Allen, N. S.; Chow, Y. S.; Thompson, F.; Jewitt, T. S.; Hornby, M. R.; Simpson, L. A. *J. Photochem. Photobiol., A* **1991**, *60*, 369–381.
(25) Inagaki, M.; Imai, T.; Yoshikawa, T.; Tryba, B. *Appl. Catal., B* **2004**, *51*, 247–254.
(26) Liang, X. H.; King, D. M.; Li, P.; Weimer, A. W. *J. Am. Ceram. Soc.* **2009**, *92*, 649–654.
(27) Hakim, L. F.; King, D. M.; Zhou, Y.; Gump, C. J.; George, S. M.; Weimer, A. W. *Adv. Funct. Mater.* **2007**, *17*, 3175–3181.
(28) King, D. M.; Liang, X. H.; Burton, B. B.; Akhtar, M. K.; Weimer, A. W. *Nanotechnology* **2008**, *19*, 255604.
(29) Liang, X. H.; Weimer, A. W. *J. Nanopart. Res.* **2010**, *12*, 135–142.

AM100279V